ELECTROMAGNETIC MODELING OF VIRTUAL HUMANS TO DETERMINE HEART CURRENT FACTORS

Hai Jiang, PhD. P.E.
Mahmood Tabaddor, PhD

RESEARCH REPORT
(DISTRIBUTION: EXTERNAL/PUBLIC)
DECEMBER 2017

UL LLC
333 Pfingsten Road, Northbrook, IL 60062-2096 USA
www.UL.com

DISCLAIMER

This report was prepared for research purposes only by UL staff. The information contained herein relates only to the products tested for the purposes of this report. UL LLC does not warrant that this information is complete or accurate or is applicable to products other than those actually tested. This report does not mean that any product referenced herein is Listed, Classified, Recognized or otherwise certified by UL, nor does it authorize the use of any UL certification marks or the UL name or logo in connection with the product or system. In no event shall UL LLC, or its be liable for any damages, loss, claims, costs, or expenses arising out of or resulting from the reliance on, use, or inability to use the information contained herein. Nor shall UL LLC, or its affiliates be liable for any errors or omissions in the report.

TABLE OF CONTENTS

INTRODUCTION

According to the survey of emergency rooms by the NEISS (National Electronic Injury Surveillance System (NEISS)), approximately 5,000 people are injured every year due to electrical shock, the passing of electric (AC or DC) current though the body. In another study, a survey of Occupational Injuries and Illnesses (U.S. Bureau of Labor Statistics Databases, Tables & Calculators by Subject, 2017), they found that over 300 workers are killed per year because of electrical shock. So there is still work to be done to help improve electrical shock safety. Though, to further advance electrical shock safety, it is important to have an understanding of how the human body interacts with an electric energy source. Yet, the necessary testing would be dangerous to humans.

Looking at standards covering electrical safety (IEC 60479-1, 2005), there are four different human body physiological effects due to electric shock. The first, and the lowest level impact, is perception. At this level, a person subjected to a low-level of current will sense the unpleasantness from the electrical energy streaming through their body but will not be injured directly from the passing of current. Once the current flow is stopped, the perception goes away with no permanent damage. However, perception may cause injury through secondary consequences. For example, the surprise feeling of being shocked may cause a person working on a ladder to fall off which could result in very serious injury or even death. The next level physiological effect of electric shock exposure is the inability to let-go. The muscles of the human body will contract and "freeze" due to the stimulus from electrical energy. If the victim is holding an electrical wire or grabbing an energized metal object, he or she may not be able to "let-go", and the electrical current will keep flowing through the human body leading to more serious damage. Considering different scenarios in terms of exposure time, health and physical condition of the human body, and current level, the consequences of "let-go" can range from minor injuries to serious injuries or even death. The current threshold above which the human body will experience the perception and "let-go" physiological effects is 0.5 mA and 5 mA, respectively (IEC 60479-1, 2005). The third level with the most complicated physiological effects is called ventricular fibrillation. Beyond a certain threshold, the current can fibrillate the heart causing it to stop pumping blood, leading to death. The current threshold to protect from ventricular fibrillation is in 20 mA in the US and 30 mA in Asia and Europe (where a 220 V is the common supply voltage). The fourth level of physiological effects is tissue burning. When the current is above 70 mA, human tissue will be burned as the electrical energy is converted into heat. All thresholds assume worst case scenario which, for electric shock, means that the body region receiving the electric shock has a wetted skin and large contact surface area with some part of the body.

Figure 1 shows the limit of electrical shock physiological effects from perception to ventricular fibrillation as described in electrical safety standards. For example, zone AC-1 covers perception effects due to exposure to current. For perception, exposure time (vertical axis) is not critical. With increasing current, then the hazard moves into zone AC-2, where the inability to let-go is the primary hazard. In this region, both current levels and exposure duration are determining factors. Clearly as the current level increases, the acceptable exposure duration starts to decrease and the possibility of more serious consequences increases. The details of the other zones can be found in (IEC 60479-1, 2005).

Most of the current thresholds for perception and "let-go" physiological effects were derived from experimental results on children and adults from different researchers, such as Dalziel (Dalziel, 1943) from the early 1900s. Over time ethical concerns and legal restrictions prohibited experiments of electrical shock on children and even adults. One alternative approach to physical testing has been electrical circuit analysis to represent the internal electrical behavior of the human body. By modeling the human body as lumped electrical (resistors and capacitors) components and considering the hazardous source as current or voltage sources, tractable calculations can be carried out to estimate certain measures of the hazards of electric shock, such as the touch current. The advantages of using circuit analysis are the ease of implementation implement and their simplicity. The downside is that the simplifications come at the cost of the detailed insight necessary to help advance electric shock safety.

Over the last few years, advances in technology, specifically imaging technology and engineering modeling software, are now making detailed 3D digital human bodies practically available for understanding the internal effects of exposure to electrical shock, or electromagnetic energy in general. By using accurate and detailed 3D anatomical virtual human body models, which can be obtained from high resolution medical imaging scans, computational electro-pathology can now become an important tool in advancing electrical safety.

In this paper, some of the recent work using 3D anatomical human body modeling for studying electrical shock hazards and electro-pathology are reviewed. In our research, we build and assess the accuracy and usefulness of such a 3D virtual human body model by determining one measure of electric shock hazard, the heart current factor (HCF), and comparing results with values found in published research and safety standards documents.

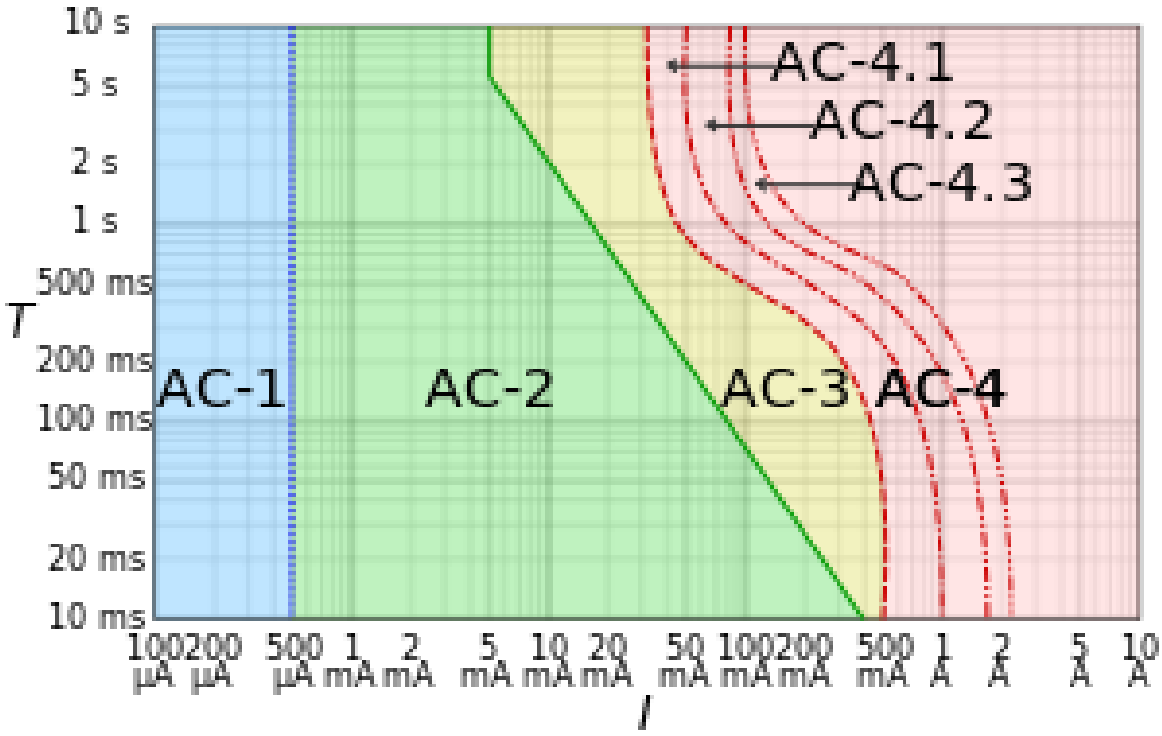

Figure 1 Conventional time/current zones of effects of AC currents (15 Hz to 100 Hz) on persons for a current path corresponding to left hand to feet

A BRIEF REVIEW OF ELECTRIC SHOCK MODELING

When the human body is subjected to electrical currents and fields, it has an electrical response that is greatly determined by the electrical properties of biological tissue. Therefore, an electrical model of the human body is required though the complexity of the level of modeling is dependent upon the practicalities of what is possible and what is being sought. From the simplest level, there is a circuit based modeling to the most comprehensive approach, solving of the full equations of electromagnetics known as Maxwell's equations. In the field of electrical shock safety, circuit modeling has been also used for a long time with one example being establishing the acceptable leakage current levels. With simple models come simple insights. To understand potential safety issues with actual products, then it will be necessary to resort to more insightful modeling techniques. With the tremendous advances in computing technology and software, now it is possible to accurately estimate more challenging electromagnetic effects: as one example, the wireless radiation level at radio frequencies as researchers try to understand potential hazards associated with wireless radiation hazards. Though there are multiple ways to categorize modeling, from quasi-static to dynamics, low to high frequency ranges, uncoupled to coupled, a simple characterization from circuit analysis to a full 3D electromagnetics analysis is followed here. Next, we present a brief review of the some recent research covering the use of mathematical modeling in electric shock.

Electrical Circuit Modeling

Although there are some limitations, circuit modeling using electronic circuit components has served as a simple yet effective approach for engineers to mathematically model and analyze electric shock safety in terms of human body impedance. Such circuit models have been widely used in national and international safety standards such as UL and IEC in determining touch current limits. Figure 2 shows the human body impedance model (IEC 60479-1, 2005) used in a device designed for measuring reaction current[1]. The 1500 Ω resistor and the 0.22 μF capacitor represent the skin only impedance and the 500 Ω resistor represents the internal human body impedance. Together they comprise the human body impedance model. The 10 kΩ resistor and the 0.022 μF capacitor are not

[1] Reaction current is defined as a threshold current value, above which a substantial portion of the population may react involuntarily to the sensation of current.

part of the base human body impedance but represent another complexity of a real human body, the frequency dependence of the human body impedance.

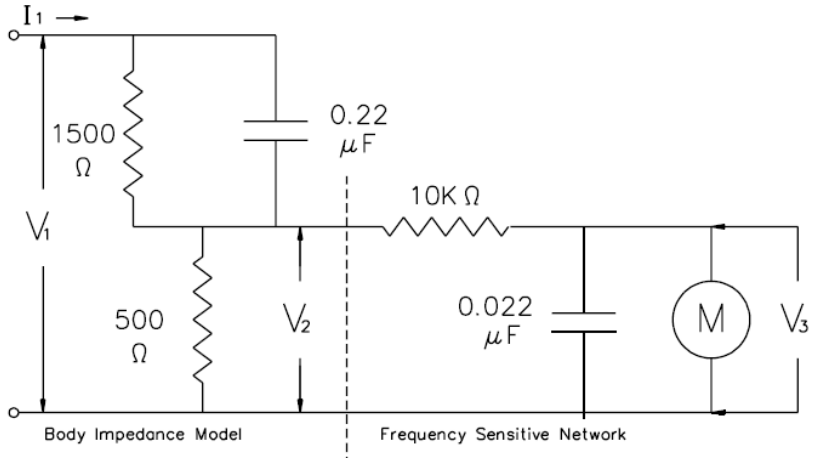

Figure 2 Human body impedance circuit model (IEC 60479-1, 2005)

A different circuit model for safety standards (IEC 60479-1, 2005) is shown in Figure 3. The Z_{S1} and Z_{S2} are the skin impedance consisting of a 1500 Ω resister and a 0.22 μF capacitor. The Z_i represents the internal human body impedance of 500 Ω and is placed in parallel with the frequency dependent network of 10 kΩ resistor and the 0.022 μF capacitor. Z_T denotes the total human body impedance.

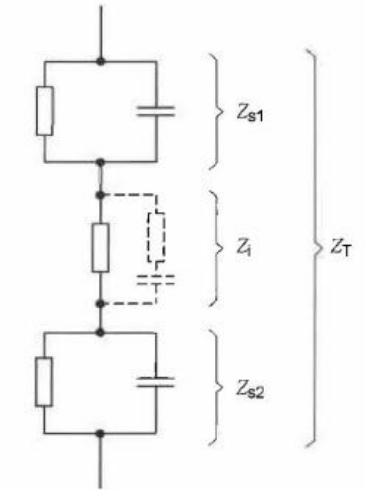

Figure 3 Alternate impedance model of human body (IEC 60479-1, 2005)

Another IEC standard (IEC 60990, 2016) recommends a similar circuit-based human body impedance model for providing guidelines on how to measure the touch current for different physiological effects such as reaction and Let-go[2]. The network for measuring the let-go current is shown in Figure 4 which is similar to that shown in Figure 2. The difference between the two networks is in the particulars of the frequency sensitive network while the human body impedance remains the same.

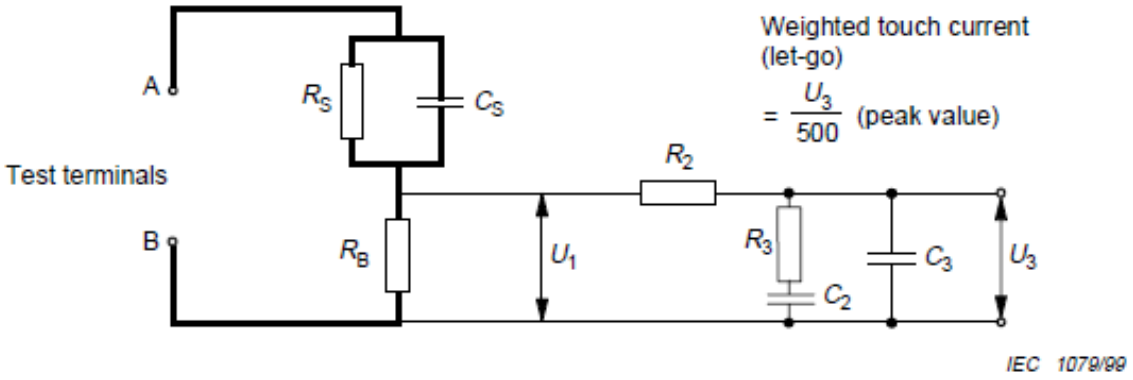

R_S	1 500 Ω	R_3	20 000 Ω
R_B	500 Ω	C_2	0,0062 µF
C_S	0,22 µF	C_3	0,0091 µF
R_2	10 000 Ω		

Figure 4 Circuit for measuring touch current for Let-go effects

A more distributed internal impedance model of human body is also given in the standards (IEC 60479-1, 2005) and shown in Figure 5. It is still a circuit based model. A percentage of the impedance is provided for different body parts including limbs and torso in relation to the internal impedance from hand to foot. For example, the center of the chest has 5.2% of the total internal impedance from hand to foot. However, it is noted that this only models the internal human body as resistance without any reactance components. The accuracy and the applicability of the results are very limited.

[2] Threshold of let-go current is the maximum value of touch current at which a person holding electrodes can still let go of the electrodes.

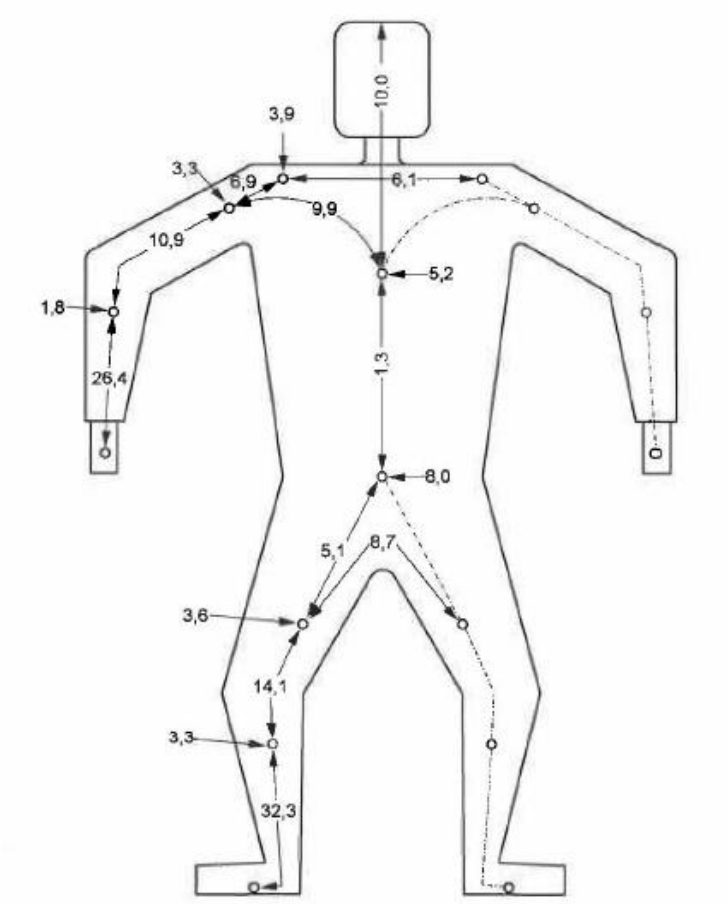

Figure 5 Internal body impedances for key pathways (IEC 60479-1, 2005)

In some recent research (Santis & et al, 2011), another circuit model was proposed as shown in Figure 6. This circuit model was derived from measurement data on a population of adults. Because the circuit model is derived from experimental results, it is important to understand how the human body impedance was measured. In this research, they measured the human body impedance using both a network analyzer and impedance analyzer on a population consisting of 30 adult males and 25 adult females. The impedance analyzer setup was used to measure the impedance below 1 MHz, and the network analyzer was used to measure the impedance from 1 MHz up to 110 MHz. One setup used in their experiment was with barefoot subjects touching a grasping contact with wet, saline skin which was in general considered as the worst case scenario in the field of electrical shock. Figure 7 shows the (Santis & et al, 2011) comparison of human body impedance between the experimental results and equivalent circuit networks. The line labeled IEC network is represents the circuit model previously discussed from the IEC standards.

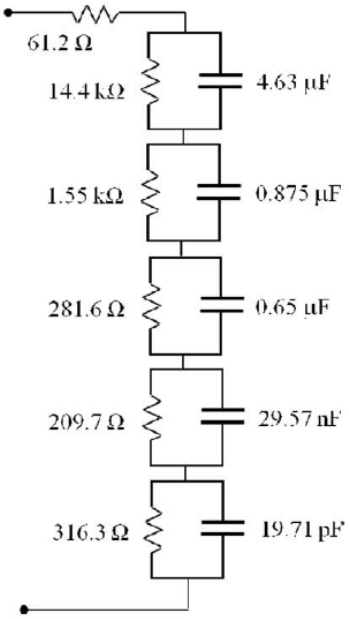

Figure 6 Human body impedance network (Santis & et al, 2011)

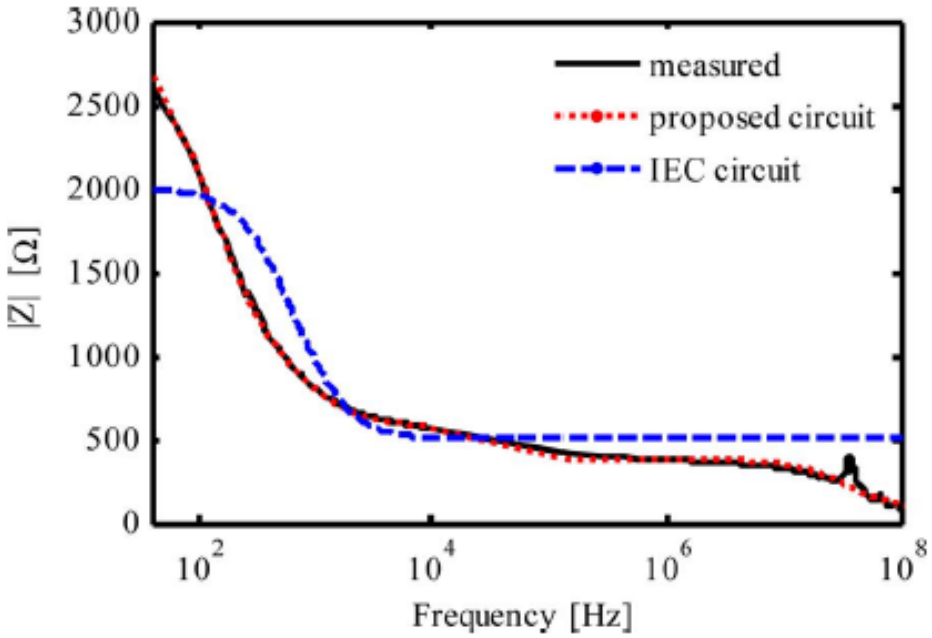

Figure 7 Measured and fitted human impedance (Santis & et al, 2011)

There have been some insights provided by circuit based models of human electrical response to external electrical current. Some complexity such as multiple components, consisting of resistance and capacitance, in parallel and in series, has been added to improve the accuracy and range of applicability of the models. It is clear that any useful human body model would need to account for electrical properties of the body that have dependence upon the frequency of electromagnetic source.

3D Electromagnetics Modeling

Generally, full 3D electromagnetics modeling has been used for high frequency applications. However, electric shock is considered an extremely low frequency (ELF) event. When a grounded human touches an energized objects (or vice versa) at 50 Hz or 60 Hz and a conductive loop is formed through the body, contact current flows through the body. It is generally assumed that this is the main effect and so for that reason circuit models have been popular. By far, the largest use currently of 3D human body models for electromagnetic (EM) modeling is to estimate high frequency electromagnetic fields and the radiation generated by electronic devices and their interaction with a human. However, for electric shock, once we introduce the complexity of the human body, with all the individual tissues and organs, with their irregular shapes and volumes, then it is necessary to resort to 3D electromagnetics analysis.

In (Werner & et al, 1998) and (Sachse & et al, 2000) an anatomical model was created based on a data set of human body medical scans subjected to advanced image and graphical processing. The anatomical model consisted of 370 million cubic voxels, each voxel having a size of 1 mm x 1 mm x 1 mm. Each voxel were assigned to one of forty different tissue or organs, such as, muscle, fat, bone, marrow, skin, and blood, to name a few. The human body model was used to solve the forward problem of electrocardiography, which mainly consisted of determining the electric potential field within the torso arising from cardiac sources. The cardiac sources represented measurements taken from the excitation process within the heart.

In (Tarao & et al, 2012), the researchers performed numerical calculations of internal electric fields at 60 Hz contact currents for the typical hand to foot pathway using a 3D human model. For the numerical calculation, an adult male human model (known as Duke, 1.74 m in height and 70 kg in weight) was used, which consisted of 77 tissues or organs (Christ & et al, 2010) with each voxel assigned a conductivity value corresponding to a given tissue. At low frequencies, the electrical resistivity of the body is generally more dominant than the capacitive components. Therefore, the permittivity of the tissues was ignored in their calculation. A voxel size of 2 mm, which resulted in

approximately 8.6 million voxels in total, was used. An in-house software/program based on scalar potential finite difference was used for the numerical calculations, and the results were compared with those obtained by the finite element method. It was shown the size of the voxel is a critical factor in how well the two methods agreed.

As noted, a typical current pathway between the hand and foot was used in their study, in which two electrodes were attached, one on the palm of the left hand and one on the sole of the left foot. A voltage source at 60 Hz was applied across the electrodes. This was the base case. Next, they performed additional calculations varying tissue conductivity and contact area, and compared the results with the base case. For the base calculation, the electrode surface area in contact with the left palm was 130 cm^2, corresponding to a 'large' size defined in the (IEC/TS 60479-1). This contact area was assumed to represent the grasping of an electrode with the hand.

Figure 8 shows one example of the calculated internal electric field distribution based on vector-averaging of the fields for the base case, the directions of which are represented by a unit vector, and the magnitudes of which are represented in a logarithmic scale. The electric fields were high on the current pathway at the left arm, torso and left leg, and were low at the head and the extremities without the electrode. Furthermore, the electric fields in the left arm were clearly larger than those in the torso.

In (Chan & et al, 2013), they investigated the in-situ electric field due to low-frequency contact current along with the Specific Absorption Rate (SAR) due to high frequency contact currents for the grounded and ungrounded human models (Figure 9). The reference level for the general public was used as the source value of the contact current, and the computed in situ electric field and SAR distributions were compared with the basic restriction imposed by the ICNIRP guidelines (International Commission on Non-Ionizing Radiation Protection[3]).

[3] http://www.icnirp.org/

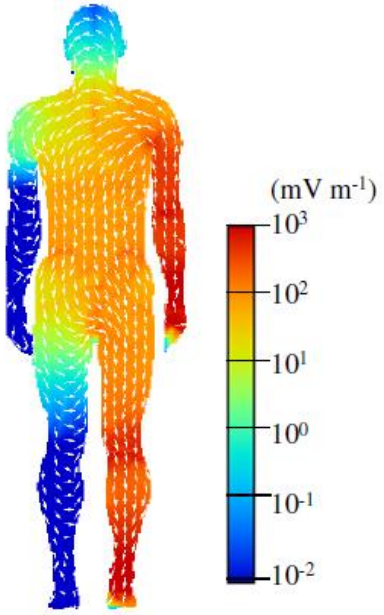

Figure 8 Electric human body field distribution for left hand to left foot pathway (Tarao & et al, 2012)

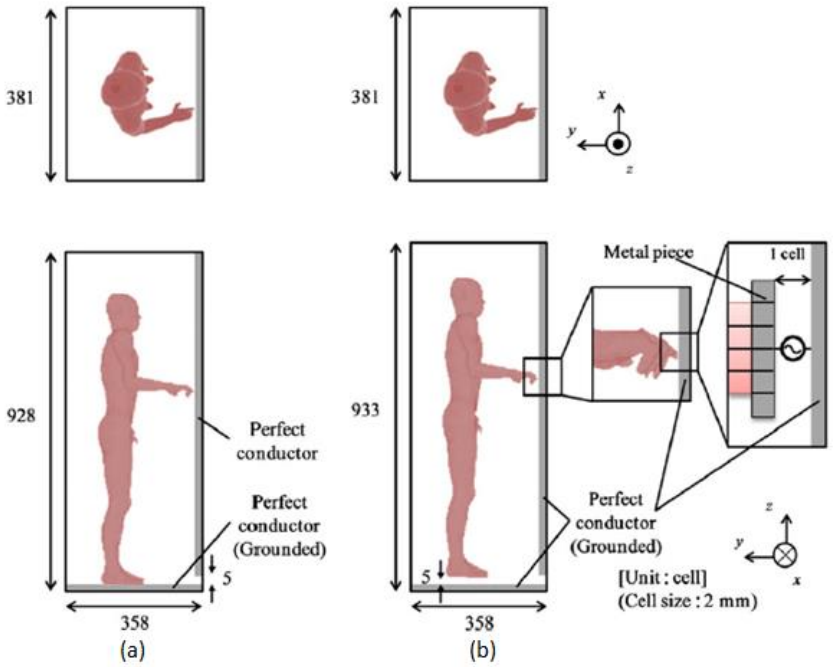

Figure 9 Top view and the side view of the (a) grounded anatomical human body model, and (b) ungrounded anatomical human body model and voltage source modelling for the analyses of the contact currents (Chan & et al, 2013)

A 3D anatomically based model named TARO (Nagaoka & et al, 2004) was used in another study. In their full-wave analysis, the dielectric constants and conductivities of the human tissue were set based on the data from Gabriel (Gabriel & et al, 1996) which was the main source for human tissue electric properties in our research. The dielectric constants and conductivities for muscle, fat, and skin at 10 kHz, 1 MHz and 100 MHz used in our studies are listed in Table 1.

Table 1 Dielectric properties of human tissue

		10 kHz	1 MHz	100 MHz
Muscle	σ (S m^{-1})	0.34	0.50	0.71
	ε_r	25 909	1836	66
Fat	σ (S m^{-1})	0.043	0.044	0.068
	ε_r	911	51	13
Skin	σ (S m^{-1})	2.0×10^{-4}	0.013	0.49
	ε_r	1134	991	73

In the Nagaoka study, the induced electric field (in situ electric field) was computed for a wide frequency range from 10 Hz to 100 MHz. A magneto-quasi-static approximation finite-difference time-domain (FDTD) method was used for the frequency range between 10 Hz to 1 MHz. The conventional FDTD was used for frequency range between 1 MHz to 100 MHz.

The induced electric field was computed for different human body tissues and organ, and the results were compared with the basic restriction provided in ICNIRP as shown in

Table 2. The reference level in general was typically more conservative than the induced electric fields and SAR values given for basic restrictions. In their comparison, some discrepancy was found between the computed results from the reference level and the basic restrictions. The computed results showed that the induced electric field in the fat and the muscle exceeded the basic restrictions in the standard at frequencies below 1 MHz.

Table 2 Comparison of the maximum induced electric field (Chan & et al, 2013)[4]

Frequency (Hz)	10	100	1 k	3 k	10 k	100 k	1 M	10 M
Reference level (mA)	0.5	0.5	0.5	0.6	2	20	20	20
			Basic restriction (V m^{-1})					
CNS tissue of the head	0.01	0.04	0.4	0.4	1.35	13.5	135	1350
All tissues of the head and body	0.4	0.4	0.4	0.4	1.35	13.5	135	1350
			Induced electric field (V m^{-1})					
Brain	0.02	0.006	0.005	0.006	0.018	0.16	0.12	0.53
Spinal cord (head)	0.008	0.004	0.003	0.003	0.01	0.074	0.042	0.8
Spinal cord	0.36	0.28	0.25	0.29	0.9	7.7	5.61	2.8
Heart	0.39	0.27	0.24	0.25	0.72	5.18	3.54	2.1
Fat (excluding finger)	5.78	5.08	4.72	5.53	18.2	177	152	100
Muscle (excluding finger)	5.43	4.68	4.31	5.06	16.6	161	134	88

More recently, researchers (Chan & et al, 2014) extended their computational investigation to a realistic child model for in-situ electric field due to low-frequency contact current and specific absorption rate (SAR) due to high-frequency contact currents. They compared the child results with those in the adults form their previously cited study.

Similarly, the results were computed for frequencies from 10 Hz to 110 MHz and compared with the basics restriction in ICNIRP. Figure 10 shows the child model used in the simulation for grounded and ungrounded cases. The results show that the in-situ electric fields and SAR in the child model are found to exceed the corresponding values in the adult. At the fingertip, the electric field and SAR due to contact currents, both at the ICNIRP reference levels and IEEE Maximum Permissible Exposures[5], are well beyond the corresponding basic restrictions. The largest difference was observed in the spinal tissue, and the smallest effect was seen in the heart.

[4] CNS denotes the central nervous system.

[5] C95.1-2005 - IEEE Standard for Safety Levels with Respect to Human Exposure to Radio Frequency Electromagnetic Fields, 3 kHz to 300 GHz.

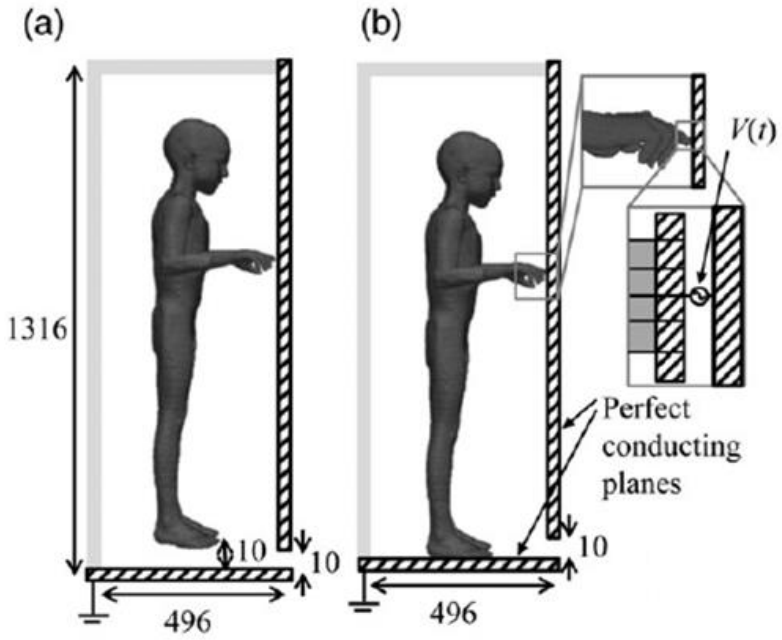

Figure 10 Modelling of (a) ungrounded child touching a vertical metallic plane and (b) grounded child touching a vertical metallic plane

Another group of researchers ((Tarao & et al, 2009) (Freschi & et al, 2013)) applied computational electromagnetics to a full human body model to study the heart current factor. Some discrepancies were found between their results and the values listed in IEC standards. It was explained in the reports that the tissue property might be the cause for such discrepancies and recommended further investigation. In this paper, the heart current factor will also be studied and compared with previous investigations and data from IEC safety standards.

HEART CURRENT FACTOR

Ventricular Fibrillation (VF) is one of the most dangerous physiological effects due to electrical shock which may lead to death if the current is over the limit and with prolonged exposure. Table 3 (IEC 60479-1, 2005) shows the threshold of the heat current factor (HCF) and its relationship with time. The HCF acts as a indicator for VF. It is noted that these thresholds and guidelines are set for a current path from left hand to both feet as the baseline. These thresholds were developed by the Maintenance Team 4 (MT 4) of the larger IEC Technical Committee 64 (TC64) based on previous research studies and experiments on animals by applying extra safety factors for human body versus animals. Once the current pathway changes, these thresholds will change accordingly as the amount of current, or current density, passing through the heart will differ. With different pathways, the heart current factor is defined and permits the calculation of currents I_h through paths other than left hand to both feet which represent the same danger of VF as that corresponding to I_{ref} left hand to both feet baseline.

$$I_h = \frac{I_{ref}}{F}$$

where

I_{ref} *reference body current for the path left hand to feet from IEC 60479-1*

I_h *body current for specific path given in Table 3*

F *heart-current factor given in Table 3*

Table 3 HCF for different current pathways through the body (IEC 60479-1)

Current path	Heart-current factor F
Left hand to left foot, right foot or both feet	1,0
Both hands to both feet	1,0
Left hand to right hand	0,4
Right hand to left foot, right foot or to both feet	0,8
Back to right hand	0,3
Back to left hand	0,7
Chest to right hand	1,3
Chest to left hand	1,5
Seat to left hand, right hand or to both hands	0,7
Left foot to right foot	0,04

For example, the VF threshold for the particular pathway from right hand to feet is higher than left hand to feet, and the value is equal to $\frac{I_{ref}}{0.8}$ which is 25% more than the reference pathway. On the other hand, the pathway of current from the chest to left hand or right hand is more dangerous than reference pathway with the threshold reduced by a factor of 1.3 or 1.5, respectively. These values were derived and incorporated into the IEC standard almost 30 years ago.

Collecting measurements of heart current factors for ventricular fibrillation threshold on live subjects is dangerous. However, with the state-of-art numerical modeling method and more accurate human body models, these values of heart current factor can be calculated and compared for different pathways. The advantage of looking at something like heart current factor is that despite the challenge in getting accurate electrical properties for the human body models, the relative difference in the threshold for the pathways is still insightful.

For the research in this report, a male adult human body called Duke (version cViP 3.0, from IT'IS Foundation) was used. The cViP3.0 models have more than 300 tissues and organs and a voxel resolution of $0.5 \times 0.5 \times 0.5$ mm throughout the entire body. Some body segments can even be rotated for the Duke model to create more realistic positions. As shown in Figure 11, the left forearm was bent 90 degrees at the elbow to create a pose holding the hot electrodes comparable to actual pose of an experiment. Figure 12 shows another pathway. In these simulations, the mesh size for the electromagnetic analysis was 2 mm for all x, y and z directions to balance the opposing constraints of simulation time and accuracy.

Nine different models were run simulating the current pathways shown in Table 3. Two types of electrodes were used to create contact with the human body: a cylindrical electrode with grasping hand contact, and a square patch electrode for chest and back contact. The cylinder had a cross-sectional radius of 40 mm and a length of 500 mm. The square patch had a length and width of 100 mm. Both of the electrodes were simulating a large contact area of 10,000 mm^2 as described in electrical safety standards (IEC 60479-1, 2005). The larger contact leads to a lower body impedance and higher body/contact current. A voltage source with 110 V was used to simulate the residential electrical power supply in the United States. The maximum current density on the heart muscle and heart lumen was taken and used as the value for comparsion.

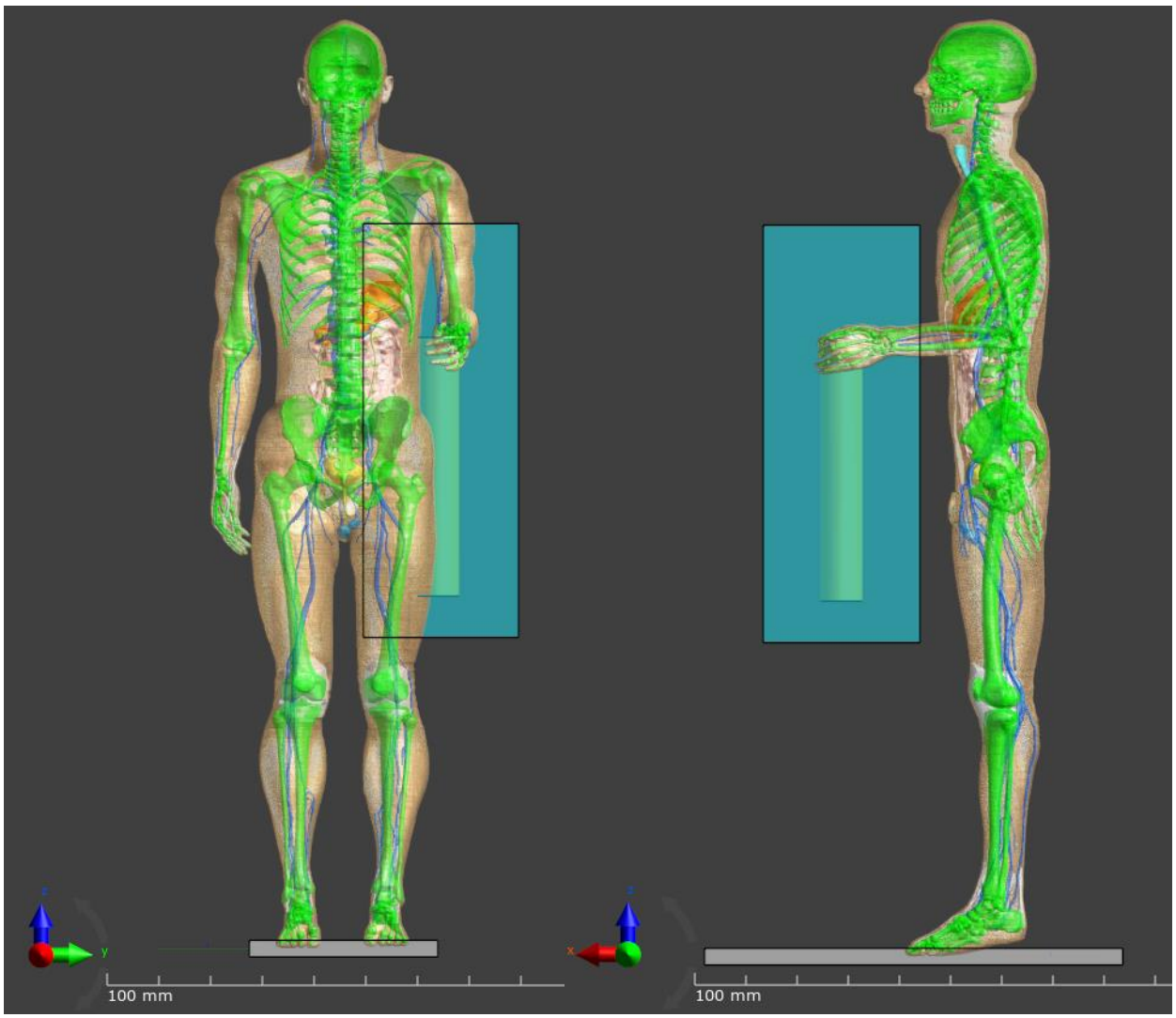

Figure 11 Human body model with pathway from left hand to both feet showing front view (left) and side view (right)

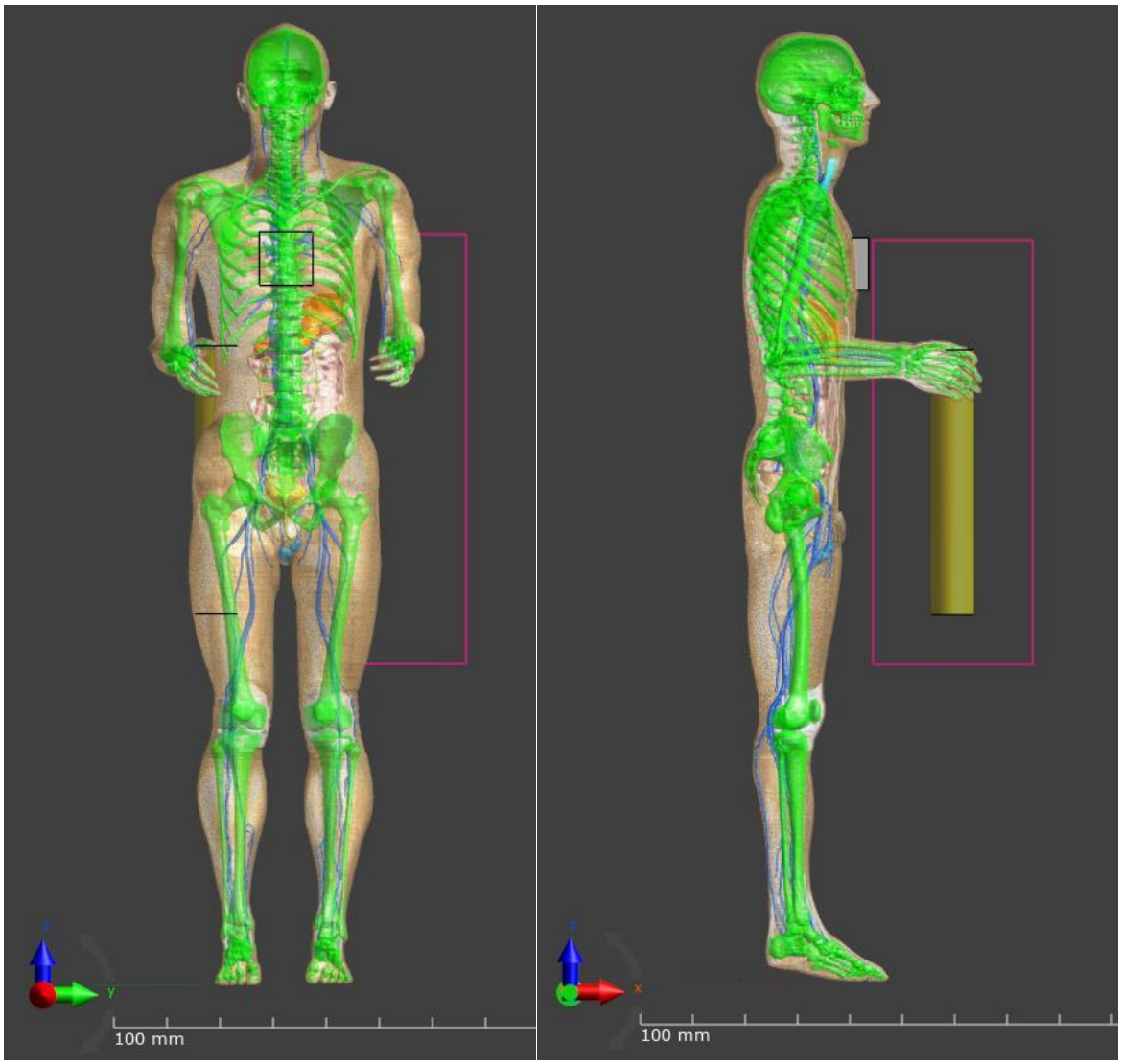

Figure 12 Human body model with pathway from left hand to a point on the chest showing front view (left) and side view (right)

By defnition, the HCF compares the electric field strength (or current density) in the heart for a given current path to the electric field strength (current density) in the heart for a touch current of equal magnitude flowing from left hand to feet (reference pathway). Since a voltage source was being used in our simulation instead of current source as stated in the definition, a transformation factor had to be applied to the results of the current density to create a consistent definition of heart current factor. Assuming body current, and maximum current density on the heart were I_{ref} and J_{ref}, respectively, the touch voltage was $Z_{body} \times I_{ref}$.

The definition of the HCF states that the touch current between the interested pathway and reference pathway should be the same. For our study, the voltage was set the same for all cases and a linear transformation carried out to help derive the heart current factor for each pathway. It is noted that linear transformation can be made because the numerical equations are linear between the input and output. For the interested pathway, the body current is I_h and the touch voltage is $Z_{body1} \times I_h$ where Z_{body1} is the body impedance of the interested pathway. By definition $I_h = \frac{I_{ref}}{F}$ with the detailed approached shown in Table 4.

Table 4 Derivation of HCF for equal voltage source

		Voltage	Body Current	Max current density on heart
	Reference	$Z_{body} \times I_{ref}$	I_{ref}	J_{ref}
	Interested	$Z_{body1} \times I_h$	I_h	J_{ref}
x F	Interested	$Z_{body1} \times I_h \times F$	$I_h \times F$	$J_{ref} \times F$
	Interested	I_{ref}	I_{ref}	$J_{ref} \times F$
x $1/Z_{body}$	Reference	I_{ref}	$I_{ref} \times 1/Z_{body}$	$J_{ref} \times 1/Z_{body}$
x $1/Z_{body1}$	Interested	I_{ref}	$I_{ref} \times 1/Z_{body1}$	$J_{ref} \times F \times 1/Z_{body1}$
Ratio from the above two eq.		1	$\frac{Z_{body}}{Z_{body1}}$	$F \times \frac{Z_{body}}{Z_{body1}}$

The goal was to derive the max current density with an identical voltage source value. As shown in the last row in Table 4, the heart current factor can be found by taking the ratio of the max current density on the current between the interested pathway and the reference. However, as seen in Table 4, there is a transformation factor $\frac{Z_{body}}{Z_{body1}}$ to be divided to retrieve the final factor F.

RESULTS

A constant voltage source of 110 V was applied on the Duke model for 10 different pathways using the EM solver (Sim4Life software[6]). Body current was calculated by integrating the cross section current density of the forearm. Impedance was then calculated using Ohm's Law. Based on the previous derivation described in the previous section, the HCF was obtained. Figure 13 and Figure 14 show the typical current density distribution of the cross section through the heart for two different pathways. With these human body models, it is possible to gain detailed insight into the current density distribution in a single organ or throughout the body.

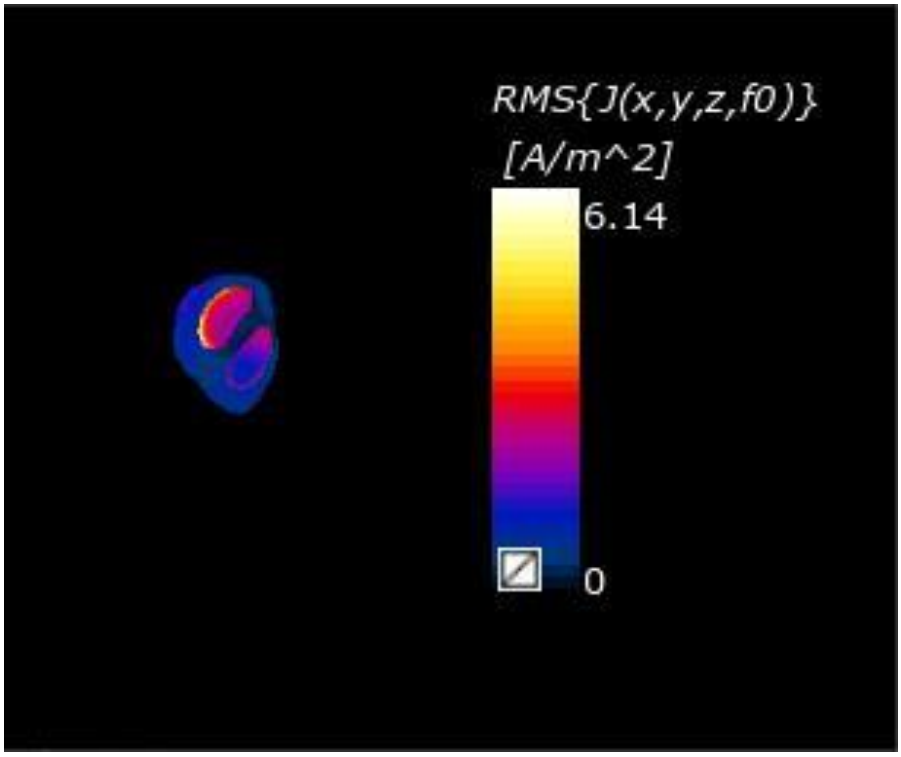

Figure 13 Current density distribution in cross section of heart for pathway of left hand to both feet

[6] https://www.zurichmedtech.com/sim4life/

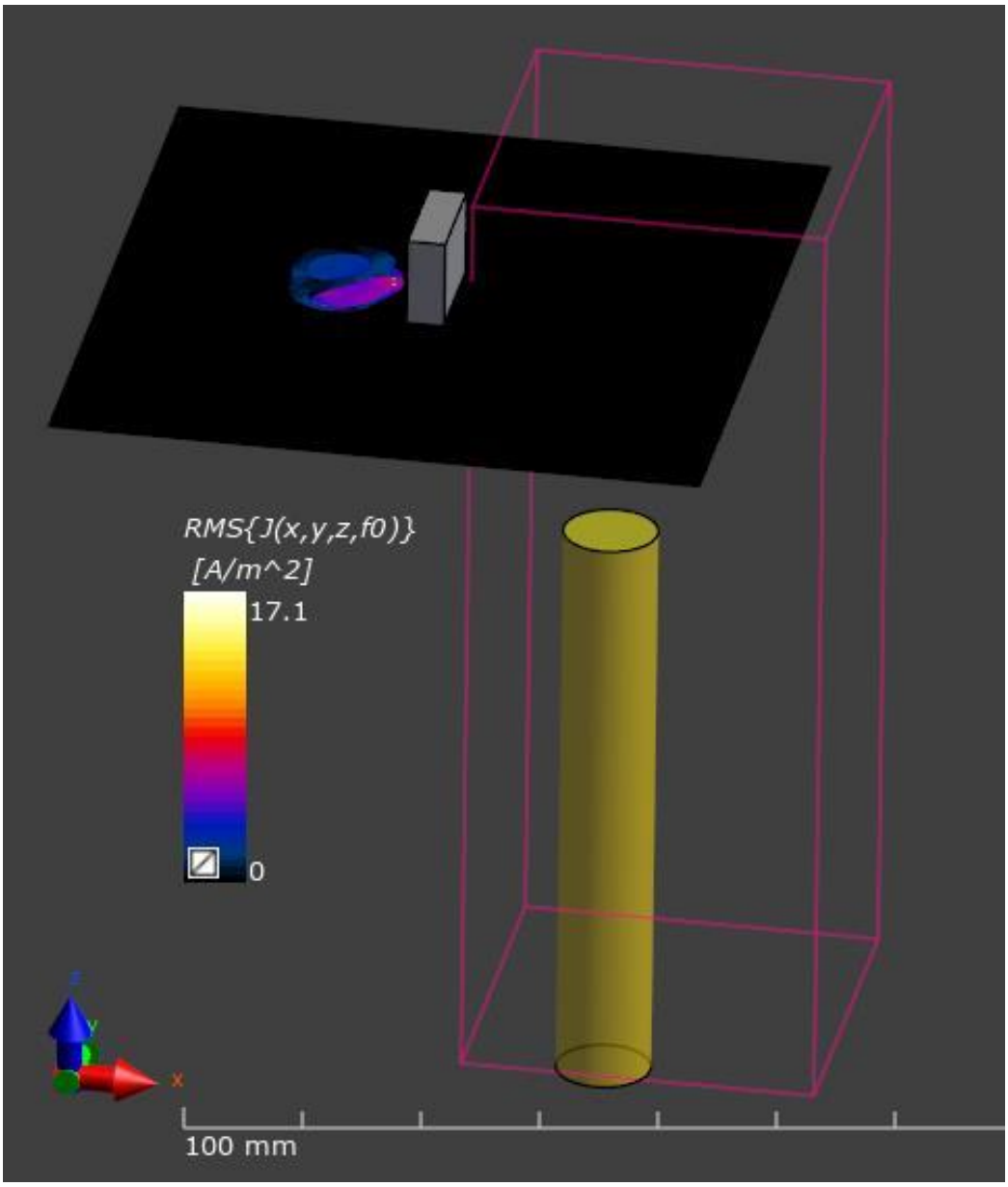

Figure 14 Current density distribution in cross section of heart for pathway from right hand to chest

Table 5 shows the modeling results from the different pathways for body current, body impedance and the derived HCF along with values available in the IEC standard. It can be seen that the simulated HCF in this research (column labeled UL2017 HCF) results matches the HCF from the IEC 60479-1 well for most of the current pathways. However, discrepancy is found for pathway of left hand to right hand and from the back to right hand. For chest to either left or right hand, the relative difference comparing to the IEC standard is also noticeable.

It is seen that the greatest discrepancy is for the pathway between the hand and either the chest or back. For the pathway to the chest or back, it is anticipated that the HCF should be sensitive to the specific y axis (see Figure 11) location of the patch electrode (the direction across the left to right arm) because the patch in either cases is rather close to the heart than in other pathways. Therefore, a sensitivity study was completed to better understand the impact of the location of the patch electrode to the HCF results and the results are shown in Table 6.

Table 5 Heart Current Factor and Body Impedance for different current pathways

Passway	Voltage	Body Current	Body Impedance	UL2017	UL2017	UL2017	IEC 60479-1
	V	mA	Ohm	A/m^2	Normalized	HCF	HCF
Left Hand to Both Feet (Reference)	110	81.7	1346.39	6.14	1.000	1.0	1
Left Hand to Left Feet	110	60.0	1833.33	4.55	0.741	1.0	1
Left Hand to Right Feet	110	61.3	1794.45	4.58	0.746	1.0	1
Both Hand to Both Feet	110	57.4	1916.38	4.245	0.691	1.0	1
Left hand to Right Hand	110	67.3	1634.47	5.17	0.842	1.0	0.4
Back to Left hand	110	132.0	833.33	5.97	0.972	0.6	0.7
Back to Right hand	110	131.0	839.69	7.11	1.158	0.7	0.3
Chest to Right Hand	110	132.0	833.33	15.6	2.541	1.6	1.3
Chest to Left Hand	110	129.3	850.73	19.5	3.176	2.0	1.5
Left Foot to Right Foot	110	64.0	1718.75	0.0283	0.005	0.01	0.04

Table 6 Sensitivity study on the heart current factor for pathway back to right hand (units for y-axis are mm)

Passway Back to Right Hand (y axis)	Voltage	Body Current	Body Impedance	UL2017	UL2017	UL2017	IEC 60479-1
Y axis	V	mA	Ohm	A/m^2	Normalized	HCF	HCF
Left Hand to Both Feet (Reference)	110	81.7	1346.39	6.14	1.000	1.00	0.3
0	110	140.0	785.71	3.29	0.536	0.31	0.3
20	110	141.0	780.14	3.82	0.622	0.36	0.3
40	110	142.0	774.65	4.06	0.661	0.38	0.3
60	110	142.0	774.65	4.6	0.749	0.43	0.3
80	110	142.0	774.65	5.57	0.907	0.52	0.3
100	110	142.0	774.65	6.66	1.085	0.62	0.3
120	110	141.5	777.39	7.76	1.264	0.73	0.3
140	110	141.0	780.14	8.82	1.436	0.83	0.3
160	110	140.6	782.36	9.75	1.588	0.92	0.3
180	110	140	785.71	10.5	1.710	1.00	0.3
200	110	139	791.37	10.8	1.759	1.03	0.3
220	110	138.4	794.80	11	1.792	1.06	0.3
240	110	137	802.92	11	1.792	1.07	0.3
260	110	135	814.81	10.9	1.775	1.07	0.3
280	110	139	791.37	10.5	1.710	1.01	0.3

Figure 15 shows the graphically the results of the sensitivity study. Horizontal axis of the figure is the patch electrode's relative position where the zero position is at the middle of back between the shoulder blades. The positive on the x axis in Figure 15 represents the right side of the back and the negative values are for the left side. As expected, as the patch electrodes get closer to the heart, the HCF increases. It reaches a peak and as the patch keeps moving left over to the arm, the HCF will decrease. Comparing to the HCF value from IEC 60479-1, the HCF from back to right hand is around 0.3. Figure 15 shows the simulated HCF value is also 0.3 if the patch electrode is positioned near the right edge of the back. From this sensitivity study, it can be predicted that the discrepancy between the chest and right or left hand is able to be explained through the sensitivity study.

Finally, a streamline of the current density is presented in Figure 16 showing the position of the patch and details of current density distribution.

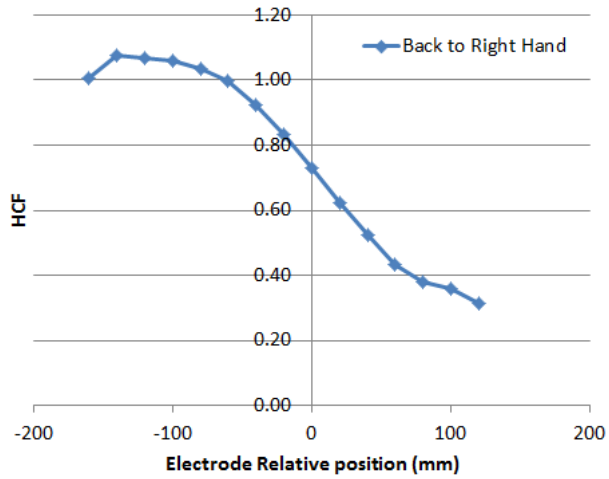

Figure 15 Heart Current Factor for different electrode position for pathway back to right hand

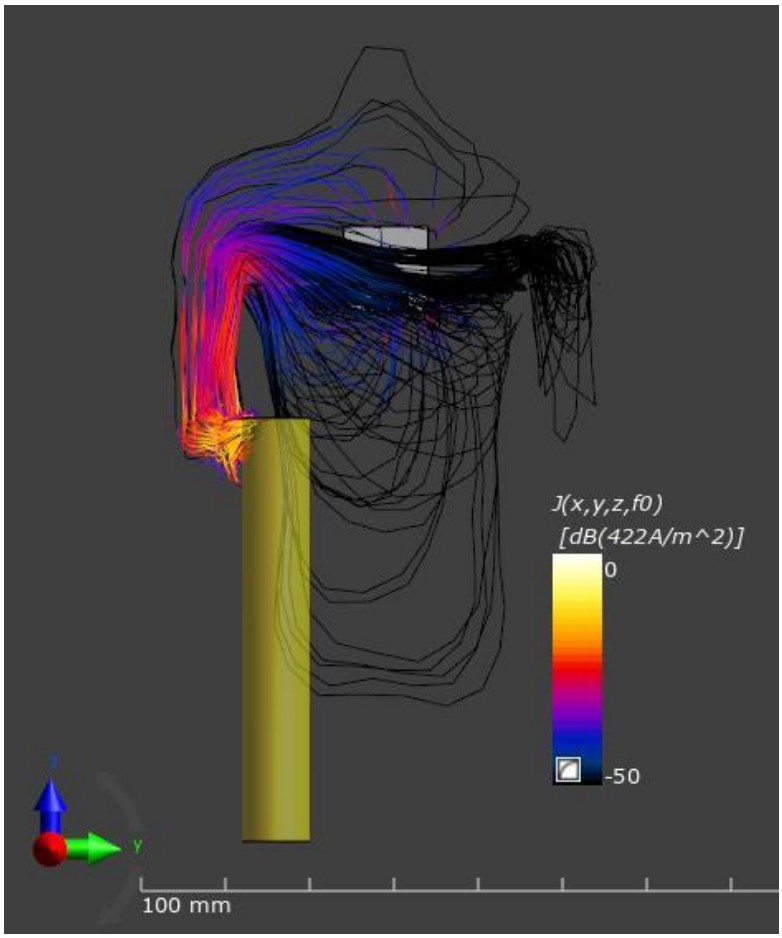

Figure 16 Streamline plot of the current density for pathway from right hand to back

HCF for certain pathways were also obtained in the study of (Tarao & et al, 2009) and (Freschi & et al, 2013). Comparison between our study (UL2017) and these other sources is shown in Table 7. Only four cases were presented in previous studies. Since the reference pathway is normalized, it will always give a result of 1.0. All studies seem to show agreement on the current pathway of left foot to right foot. In this case, the current flow is through the left leg making a turn in the pelvic region and then turning down the right leg as it moves towards the foot. Yet for left hand to right hand there is a discrepancy amongst all four cases. Yet the results from the research studies are much closer to each other than to the IEC value. Recall that an HCF less than 1 means that the pathway is less dangerous. The reasons for the discrepancy are unknown at this time.

Table 7 A comparison of HCF from different sources

Passway	UL2017	Tarao 2009	Freschi 2012	IEC 60479-1
	HCF	HCF	HCF	HCF
Left Hand to Both Feet (Reference)	1.0	1	1	1
Both Hand to Both Feet	1.0		0.66	1
Left hand to Right Hand	1.0	0.87	1.3	0.4
Left Foot to Right Foot	0.0	0.008	0.023	0.04

SUMMARY

In this research report, we detail some initial 3-D electromagnetic modeling using full human body geometry to understand the pathways for current flow during an electric shock conditions for different pathways. Though the human body models have not been fully validated, one of the key challenges being the ability to obtain accurate human tissue electric properties, we believe that these results show the promise in using such modeling to advance electric shock safety.

As for the particular results shown in this study, it is noteworthy that all the HCF predicted by the model either agree or are larger than those in the electrical safety standards. A higher predicted HCF value, for a specific pathway, as compared to the values listed in electric safety standards points to a greater danger of VF from a current flow. Mindful of the limitations of this research, these results may still be worth investigating further and in greater detail and precision.

WORKS CITED

(n.d.). Retrieved from ITIS Foundation: https://www.itis.ethz.ch/virtual-population/virtual-population/overview/

Chan, K., & et al. (2013). Computational dosimetry for grounded and ungrounded human models due to contact current. *Physics in Medicine and Biology*.

Chan, K., & et al. (2014). Computational dosimetry for child and adult human models due to contact current from 10 Hz to 110 MHz. *Radiat Prot Dosimetry*, p. 642-652.

Christ, A., & et al. (2010). The Virtual Family--development of surface-based anatomical models of two adults and two children for dosimetric simulations. *Physics in Medicine and Biology*.

Dalziel, C. (1943). EFFECT OF FREQUENCY ON LET-GO CURRENTS. *AIEE Technical Paper*, p. 43-134.

De Santis, V., & et al. (2011). Assessment of human body impedance for safety requirements against contact currents for frequencies up to 110 MHz. *Biomedical Engineering, IEEE Transactions on*, p. 390-396.

Freschi, F., & et al. (2013). Numerical simulation of heart-current factors and electrical models of the human body. *IEEE Transactions on Industry Applications* , p. 2290-2299.

Gabriel, S., & et al. (1996). The dielectric properties of biological tissues: II. Measurements in the frequency range 10 Hz to 20 GHz. *Phys Med Biol.* , p. 2251-2269.

IEC 60479-1. (2005). *IEC 60479-1; Effects of Current on Human Beings and Livestock – Part I: General.* IEC.

IEC 60990. (2016). *Methods of measurement of touch current and protective conductor current.* IEC.

Nagaoka, T., & et al. (2004). Development of realistic high-resolution whole-body voxel models of Japanese adult males and females of average height and weight, and application of models to radio-frequency electromagnetic-field dosimetry. *Phys Med Biol.*, p. 1-15.

National Electronic Injury Surveillance System (NEISS). (n.d.). Retrieved from National Electronic Injury Surveillance System (NEISS) from US CPSC: https://www.cpsc.gov/research--statistics/neiss-injury-data

Sachse, F., & et al. (2000). Development of a human body model for numerical calculation of electrical fields. *Computerized Medical Imaging and Graphics*, p. 165-171.

Santis, V., & et al. (2011). Assessment of Human Body Impedance for Safety Requirements Against Contact Currents for Frequencies up to 110 MHz. *IEEE TRANSACTIONS ON BIOMEDICAL ENGINEERING*, p. 390 - 396.

Tarao, H., & et al. (2009). Heart Current in an Anatomically Realistic Human Model due to Contact with a Low-Frequency Energized Source. *TRANSACTIONS ON ELECTRICAL AND ELECTRONIC ENGINEERING*, p. 306-308.

Tarao, H., & et al. (2012). Effects of tissue conductivity and electrode area on internal electric fields in a numerical human model for ELF contact current exposures. *Physics in Medicine and Biology*.

U.S. Bureau of Labor Statistics Databases, Tables & Calculators by Subject. (2017). Retrieved from https://www.bls.gov/data/#injuries

Werner, C., & et al. (1998). Electrical excitation of the human heart: a comparison of electrical source distributions in models of different spatial resolution. *Computers in Cardiology 1998*.